Structural Systematics. Part 4.[1] Conformations of the Diphosphine Ligands in $M_2(\mu\text{-}Ph_2PCH_2PPh_2)$ and $M(Ph_2PCH_2CH_2PPh_2)$ Complexes *

David A. V. Morton and A. Guy Orpen
Department of Inorganic Chemistry, University of Bristol, Bristol BS8 1TS, UK

Data were retrieved from the Cambridge Structural Database for 405 crystal structures containing suitable geometric data for either $M_2(\mu\text{-dppm})$ **1** (dppm = $Ph_2PCH_2PPh_2$) fragments (409 located) or M(dppe) **2** (M = transitional metal, dppe = $Ph_2PCH_2CH_2PPh_2$) fragments (274 such located). These data were analysed to examine the conformational preferences for the five-membered MP_2C_2 (or M_2P_2C) rings and the attached phenyl groups. The technique of principal component analysis was used to reduce the dimensionality of the torsion angle data set and to aid in identification of favoured conformations. The M(dppe) fragments show a preference for a twist (C_2) conformation of the MP_2C_2 five-membered ring, in which the P–C–C–P torsion angle is far from zero (typically *ca.* ±50°). In contrast the M_2P_2C five-membered rings of the $M_2(\mu\text{-dppm})$ fragments are predominantly of the envelope (C_s) conformation, with the methylene carbon out of the plane of the near-planar M_2P_2 unit, *i.e.* having the P–M–M–P torsion angle close to zero and the M–P–C–P torsion angles *ca.* ±45°. The distribution of structures indicates that in both cases the ring conformations interconvert by a pseudo-rotation pathway, similar to those observed for other five-membered ring systems, in which planar intermediates are avoided. In both **1** and **2** the two phenyl groups on each phosphorus adopt conformations typical of one- and two-ring flip mechanisms of rotation. For $M_2(\mu\text{-dppm})$ there is considerable constraint of phenyl group orientation due to clashes between phenyl groups in axial sites on the envelope M_2P_2C ring. In contrast, although weak preferences may be seen in the phenyl group conformations for the M(dppe) fragments, these arise primarily because of contacts between the phenyl groups and the ethylene hydrogens of the MP_2C_2 ring and not due to transannular Ph···Ph contacts. The implications of these observations for the design of new diphosphine ligands are discussed.

The use of diphosphines as ligands for transition metals continues to be a field of intense interest in both fundamental and applied chemistry because of the importance of the complexes they form.[2,3] The two largest classes of such complexes illustrate some of the principal reasons for this interest. The ligand bis(diphenylphosphino)methane (dppm) is particularly well suited to act as a bridging ligand between transition metals and many hundreds of complexes containing a $M_2(\mu\text{-dppm})$ unit are now known. The ability of dppm to span a wide range of metal–metal distances and hold the metal atoms in mutual proximity through the course of reactions has made it a popular choice of ligand in the development of di- and poly-nuclear transition-metal chemistry,[4] perhaps most notably in the rich chemistry of the 'A-frame' complexes with two such μ-dppm ligands. In contrast the ligand 1,2-bis(diphenylphosphino)ethane (dppe) is more well known as a chelating ligand,[5] binding to a single transition metal. Analogous complexes of closely related, but chiral, ligands with substituents at the chelate ring carbon atoms [*e.g.* *S,S*-$Ph_2PCHMeCHMePPh_2$ (chiraphos)[6] and *R*-$Ph_2PCHMeCH_2PPh_2$ (prophos)[7]] are known to be effective stereoselective catalysts.

In both these classes of complex there exist five-membered rings (M_2P_2C in the μ-dppm species, MP_2C_2 in the chelating dppe complexes) to which are attached phenyl groups at the phosphorus atoms. The conformations of five-membered rings have attracted a great deal of attention from chemists seeking to define both the likeliest conformations and the pathways for interconversion between them.[8] The frequent occurrence and the importance of such rings in metal chelate complexes (*e.g.* of ethylenediamine and dppe) has ensured that analysis of their conformational preferences has also been carried out using a number of approaches, both empirical and theoretical.[9,10] In the systems studied in this paper the orientations of the phenyl group rotors and their relationship to the conformation of the five-membered rings will also be analysed, and previous studies of di- and tri-aryl rotor systems are of relevance.[11]

In this paper we take the view (as have others) that we may learn about the favoured conformations of a (sub-)molecular fragment by examining those conformations actually observed for the fragment in the solid state in crystal structure analyses. We seek to identify the most common conformations for $M_2(\mu\text{-dppm})$ and M(dppe) fragments, and the pathways linking these conformations, and to test the conventional wisdoms of the qualitative and quantitative conformational analyses that have been advanced for such systems. In carrying out the analysis of the (torsion angle) data which describe these conformations we use the technique of principal component analysis[12] to simplify the presentation and inspection of the distribution of conformations. Parts of this work have been reported in preliminary form.[13]

Experimental

Data Retrieval.—Crystal structures containing the sub-molecular fragments $M_2(\mu\text{-dppm})$ **1** and M(dppe) **2** illustrated below were located from the Cambridge Structural Database (CSD) using the QUEST program.[14] Data for these crystal structures were retrieved from the December 1988 version of CSD in which the master data file contained 71 630 entries. The data files retrieved were screened manually and automatically

* *Supplementary data available* (No. SUP 56862, 4 pp.): Cambridge Structural Data Base reference codes. See Instructions for Authors, *J. Chem. Soc., Dalton Trans.*, 1992, Issue 1, pp. xx–xxv.

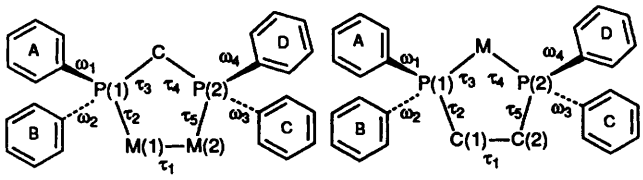

1 2

and only structures which fulfilled all of the following criteria were retained for further analysis: (*i*) *R* factor ≤0.075; (*ii*) atomic coordinates must be included in CSD; (*iii*) for multiple determinations of the same structure, only the most accurate to be retained; (*iv*) no disorder within the search fragment; (*v*) for dppe structures where the CH_2–CH_2 distance <1.5 Å were manually examined for disorder or a C=C double bond, such structures being excluded; (*vi*) for dppm, M–M vector length <3.8 Å; and (*vii*) difference between two metal–phosphorus bond distances <0.15 Å.

The final data files contained 409 μ-dppm fragments from 222 structures and 274 dppe fragments from 183 structures (see SUP 56862). The locally modified program GEOSTAT[15] was subsequently used to calculate the values of the torsion angles (τ_i, i = 1–5; ω_i, i = 1–4; see below) for each fragment. These torsion angles describe the conformations of the chelate rings and their phenyl substituents. The angles τ_{1-5} are numbered sequentially around the five-membered ring of the fragment. The four torsion angles ω_i describing the orientation of the phenyl groups were calculated as defined below, so as to fall in the range 0 to +180° according to equation (1) in which TOR(a,b,c,d) is the torsion angle calculated for atoms a,b,c,d, and $-180 \leqslant \mathrm{TOR(a,b,c,d)} \leqslant 180°$.

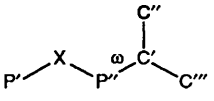

X = C for dppm
M for dppe

$$\omega = [\mathrm{TOR(X, P'', C', C'')} + \mathrm{TOR(X, P'', C', C''')} + 180]/2 \quad (1)$$

The four phenyl groups (A–D), as illustrated above, were uniquely defined by their torsion angles ψ_{1-4} as shown below and according to equation (2). Angles ψ_1 and ψ_2 were measured at P(1), and ψ_3 and ψ_4 at P(2). Angle ψ_1 associated with phenyl group A was defined to be negative, ψ_2 for ring B to be positive, ψ_3 (ring C) negative and ψ_4 (ring D) positive, thereby uniquely defining the numbering scheme used for ω_{1-4}.

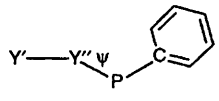

Y = M for dppm
C for dppe

$$\psi = \mathrm{TOR(Y', Y''', P, C)} \quad (2)$$

Using these definitions there are four isometric conformations (a–d) derived from the frame group of the fragments **1** or **2**, *i.e.* C_{2v},[16] with torsion angles: (a) $\tau_1, \tau_2, \tau_3, \tau_4, \tau_5, \omega_1, \omega_2, \omega_3, \omega_4$; (b) $-\tau_1, -\tau_2, -\tau_3, -\tau_4, -\tau_5, 180 - \omega_2, 180 - \omega_1, 180 - \omega_4, 180 - \omega_3$; (c) $\tau_1, \tau_5, \tau_4, \tau_3, \tau_2, \omega_3, \omega_4, \omega_1, \omega_2$; and (d) $-\tau_1, -\tau_5, -\tau_4, -\tau_3, -\tau_2, 180 - \omega_4, 180 - \omega_3, 180 - \omega_2, 180 - \omega_1$. These four sets of torsion angles describe four isoenergetic and equivalent conformations. The 409 dppm and 274 dppe fragments consequently give four times as many sets of torsion angles on symmetry expansion of the data set. The group theory of flexible systems allows the derivation[17] of the molecular symmetry group of the M(μ-dppm) and M(dppe) fragments. In addition to the C_{2v} symmetry of the central framework, the C_2 symmetry of the phenyl group rotors must be accounted for. Therefore the molecular symmetry group is $[(C_2)^2]^2 \wedge C_{2v}$. This means there are $[(2)^2]^2 \times 4 = 64$ isometric conformations for each fragment, which result from the above four sets of parameters as a consequence of 180° rotations about the P–C_{ipso} bond. In practice this means that the conformation space unit cell (which has dimensions 0–360° along each of τ_1 to τ_5, ω_1 to ω_4) contains 64 asymmetric units, four of which lie within the subcell having dimensions 0–180° in the ω_1 to ω_4 directions.

Methods of Analysis

Murray-Rust,[18] Taylor,[19] Bürgi[20] and Allen[21] and their coworkers have demonstrated the application of principal component analysis (p.c.a.) to the study of molecular conformations. In p.c.a. as applied in this paper (of the covariance matrix[12]) the objective is to construct principal components, which are linear combinations of the original parameters, that are capable of describing as much of the sample variance as possible. As many components as required may be extracted, the first being the most significant and the others sequentially decreasing in significance. The number of non-zero components that are obtained then define the 'dimensionality' of the data set. If p.c.a. is successful the components should describe the patterns in conformational variation of the fragment under investigation in an efficient way, so a multivariate set of parameters is reduced to a smaller number of underlying components. In this work the p.c.a. was performed by a subroutine incorporated in the GEOSTAT package.[15]

A more traditional approach to the conformational analysis of five-membered rings was also employed for comparison with the p.c.a. results. Equations (3) and (4) were used to obtain

$$\tau_{max} \sin \varphi = \frac{-\tau_2 + \tau_3 - \tau_4 + \tau_5}{2(\sin 36° + \sin 72°)} \quad (3)$$

$$\tau_{max} \cos \varphi = \tau_1 \quad (4)$$

phase and pucker parameters (φ and τ_{max}) describing the conformations of the five-membered rings according to the formalism of Altona and Sundaralingam.[22] Given the symmetry of the conformation space, φ values calculated on this basis of 0 and 180° correspond to C_2 symmetry twist conformers, and values of 90 and 270° to C_s symmetry envelope conformers.

In addition, histograms and scattergrams as implemented in GEOSTAT output were used to examine individual parameters and their interrelations. Other methods of defining ring conformations [*e.g.* the Cremer–Pople (CP) method[23]] were not available in GEOSTAT or other CSD software at the time of this study and for reasons described below were not applied to these and other related data. For a detailed examination of the relationship between p.c.a. and CP methods see the work of Allen *et al.*[21b]

Results

Principal Component Analysis of Five-membered Ring Conformations.—For the four-fold (C_{2v}) symmetry-expanded data set p.c.a. of all nine torsion angles τ_{1-5} and ω_{1-4} derived six significant principal components (p.c.s). Similar analysis of τ_{1-5}, the five-membered ring torsion angles, produced only two significant principal components as expected. The latter analysis is reported below and is summarised in Table 1.

The eigenvector for each principal component is characteristic of the torsion angle values for either the C_2 twist or the C_s envelope form as represented below and the p.c.s may therefore be reified in a straightforward way in this instance. However, the order of the p.c.s is different for fragments **1** and **2**. For M_2(μ-dppm) **1**, p.c. 1 explains 66.7% of the variance, and its eigenvector describes the envelope form, whereas for p.c. 2 the eigenvector describes the twist form. For M(dppe) **2**, p.c. 1 explaining 73.0% of the variance, describes the twist form, with

Table 1 Principal component analysis for τ_{1-5} for five-membered rings of $M_2(\mu\text{-dppm})$ and M(dppe)

	$M_2(\mu$-dppm)			M(dppe)		
		p.c. 1	p.c. 2		p.c. 1	p.c. 2
Eigenvalue		3.333	1.662		3.651	1.347
% Variance explained		66.67	33.24		73.01	26.94
	Standard deviation[a]	p.c. score matrices[b]		Standard deviation[a]	p.c. score matrices[b]	
τ_1	15.43	0.000	0.602	50.00	0.274	0.000
τ_2	27.99	−0.250	−0.331	40.43	−0.262	−0.212
τ_3	46.49	0.295	0.102	18.23	0.175	0.571
τ_4	46.49	−0.295	0.102	18.23	0.175	0.571
τ_5	27.99	0.250	−0.331	40.43	−0.262	−0.212
Symmetry element		C_s	C_2		C_2	C_s
Conformation type		Envelope	Twist		Twist	Envelope

[a] Standard deviation of symmetry-expanded torsion angles (°). [b] *i.e.* To obtain p.c. scores for a given structure divide each torsion angle by its standard deviation and multiply the resultant set of values by the p.c. score matrix. The plots shown in Figs. 1 and 2 show the p.c. scores calculated in this way.

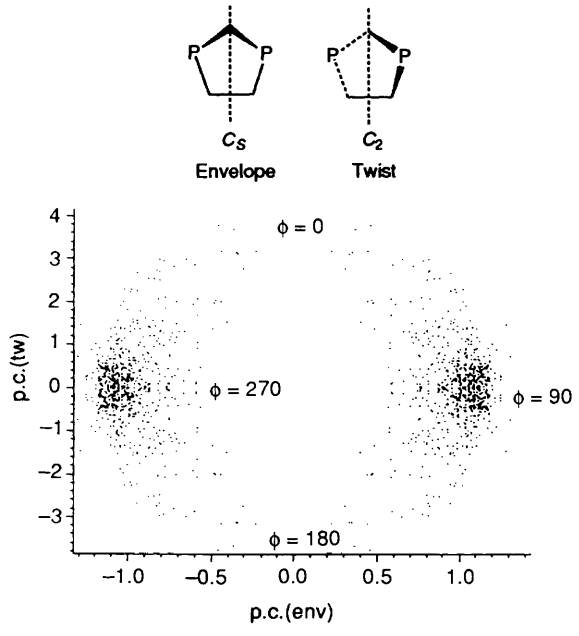

Fig. 1 Plot of principal component scores for the intra-five-membered ring torsion angles for $M_2(\mu$-dppm); corresponding AS phase angles (φ/°) are indicated

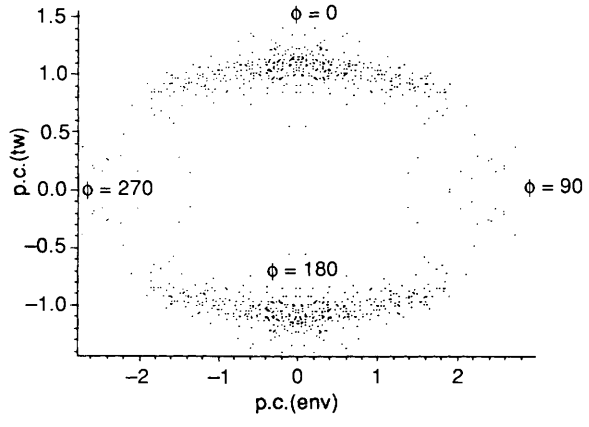

Fig. 2 Plot of principal component scores for the intra-five-membered ring torsion angles for M(dppe); corresponding AS phase angles (φ/°) are indicated

p.c. 2 describing the envelope explaining the remaining variance. We will subsequently refer to the p.c.s by their eigenvector characteristics, envelope or twist respectively: *i.e.* for $M_2(\mu$-dppm), p.c. 1 ≡ p.c.(env), p.c. 2 ≡ p.c.(tw); for M(dppe), p.c. 1 ≡ p.c.(tw), p.c. 2 ≡ p.c.(env).

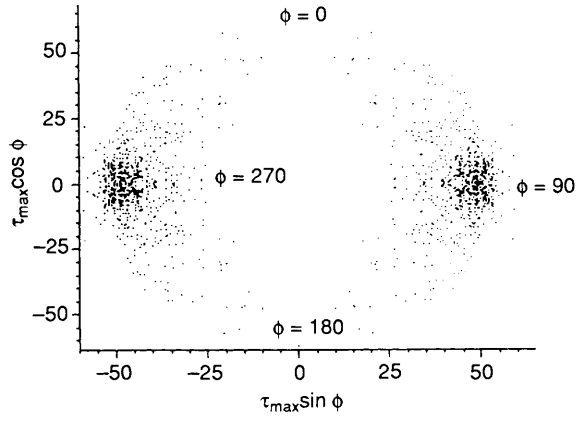

Fig. 3 Altona–Sundaralingam plot of five-membered ring conformations for $M_2(\mu$-dppm)

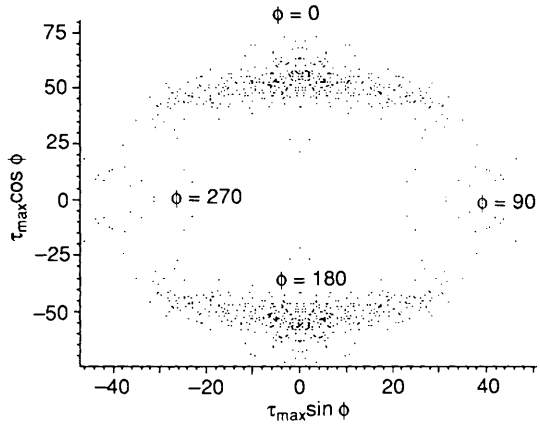

Fig. 4 Altona–Sundaralingam plot of five-membered ring conformations for M(dppe)

Figs. 1 and 2 show the distribution of conformations, in the form of scatterplots of p.c.(env) against p.c.(tw) scores, for the fragments **1** and **2**, for the four-fold symmetry expanded data sets. In these and all other scatterplots each point represents a single fragment geometry, and here the pattern of points shows the C_{2v} symmetry of this projection of conformation space. Also indicated on these plots are the locations of the conformations with Altona–Sundaralingam phase angle φ = 0, 90, 180 and 270°.

For $M_2(\mu$-dppm) fragments **1**, Fig. 1 illustrates that the points cluster at zero in p.c.(tw) and maximum extremes in p.c.(env).

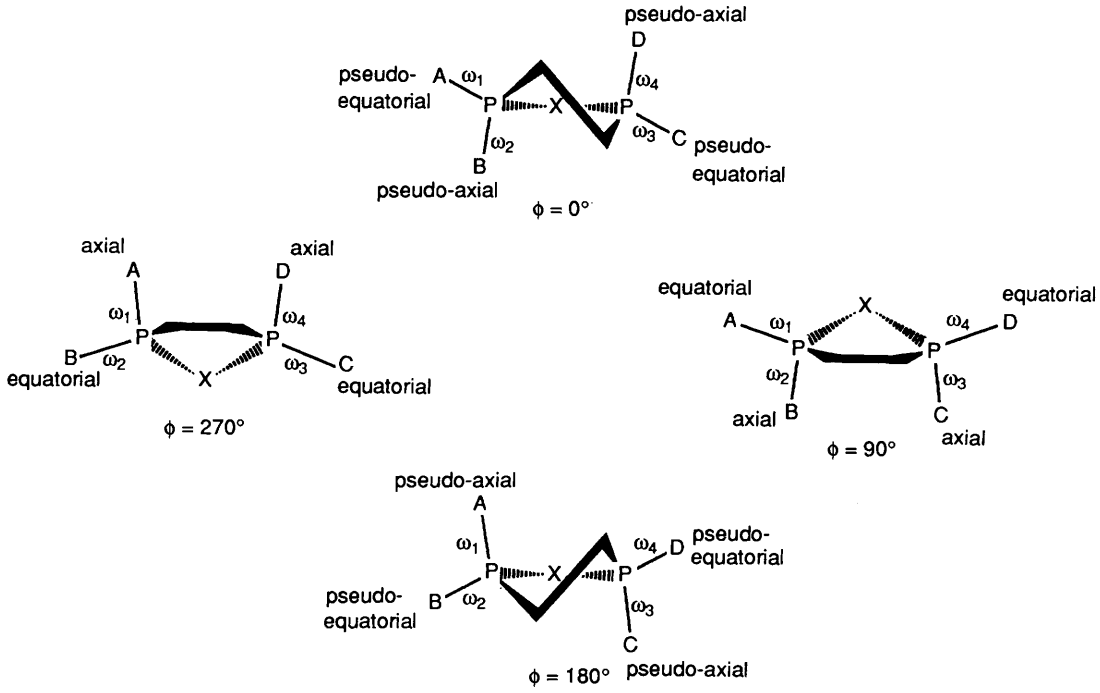

Fig. 5 Phenyl site types and torsion angle nomenclature for the five-membered ring conformations corresponding to particular φ phase angle values

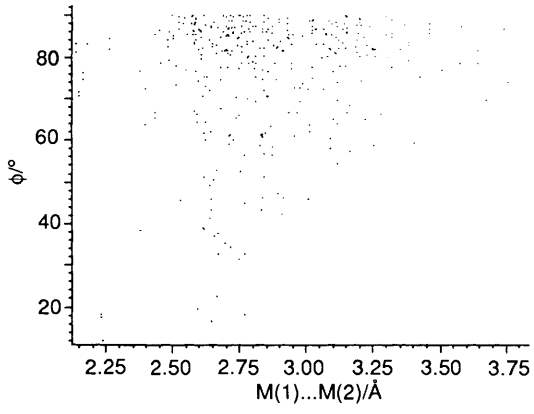

Fig. 6 Phase angle (φ) values plotted against metal–metal separation for a unique set of M_2(μ-dppm) structures

The centres of these clusters therefore correspond to envelope conformations in which the methylene carbon lies out of the plane formed by the M_2P_2 unit. In contrast, for M(dppe) fragments **2**, in Fig. 2, the clustering is about zero in p.c.(env) and at the extremes in p.c.(tw). The centres of these clusters correspond to twist (C_2) conformations of the five-membered ring of the M(dppe) fragments, the two clusters corresponding to δ (at φ = 0°) and λ (at φ = 180°) forms of the chelate rings. The p.c. score plots may be compared with the Altona and Sundaralingam (AS)[22] plots of τ_{max} cos φ against τ_{max} sin φ (see Figs. 3 and 4). Fig. 5 shows the conformations corresponding to the φ values indicated in Figs. 1–4.

Given the qualitative similarity of the p.c. score and AS plots an alternative means of obtaining an approximate phase angle φ may be suggested according to tan φ = SC[p.c.(env)]/SC[p.c.(tw)], and a pucker parameter of magnitude = $\{SC[p.c.(env)]^2 + SC[p.c.(tw)]^2\}^{\frac{1}{2}}$ may be derived, in which SC[p.c.] is the appropriate p.c. score. Murray-Rust and Motherwell[18] also exploited the similarity between p.c. score and AS plots in order to reify the p.c.s, in a similar manner. The similarity of the p.c. score and AS scatterplots is reminiscent of the similarities observed by Allen *et al.*[21b] in comparing p.c. score and Cremer–Pople plots. In all three approaches the two-dimensionality and symmetry of the conformation space of five-membered ring systems is readily appreciated. The main benefit of p.c.a. is in its greater flexibility, since it will allow inspection of data sets of any dimensionality, and also analysis of data sets including parameters other than torsion angles or displacements from ring mean planes. It is for this reason that we will use p.c.a. in this paper and others on more complex chelate and macrocycle ring conformations[24]. In the remainder of the paper we make use of the AS phase angle φ as a convenient means of indicating or defining a subset of the entire conformation space. We note that we could equally well have used the p.c. scores to achieve the same ends.

One disadvantage of p.c.a. is that the chemical significance of the components is not always easily appreciated, although as explained above this is not a difficulty in the present study. In unfavourable cases (*i.e.* when parameters show weak or zero correlation) p.c.a. may be less effective in reducing the dimensionality of a data set. Thus in this study no reduction in the four-dimensionality of the phenyl rotor projection of the data set is achieved by p.c.a. This is understandable given the periodic, rather diffuse and weakly correlated distribution of conformations shown below. It should be noted that the Altona–Sundaralingam and the Cremer–Pople formalisms also cannot provide any description of phenyl group conformations in respect of their rotation about the P–C_{ipso} bond.

Five-membered Ring Conformations.—Figs. 1 and 3 show that the M_2(μ-dppm) fragment preferentially adopts envelope C_s conformations defined by φ = 90 and 270°; the points cluster about these regions fairly tightly. In contrast, Figs. 2 and 4 show that the M(dppe) conformations are generally of a twist C_2 form, favouring φ near 0 and 180°, but their distribution is slightly more spread. This is demonstrated by the observations that for M_2(μ-dppm), 74.5% of the conformations lie in the regions 90 ± 18 and 270 ± 18°, while for M(dppe) 65% of the conformations lie in the region 0 ± 18 or 180 ± 18°. Note that these values of φ correspond to conformations close to the ideal envelope (for **1**) or twist (for **2**) but include conformations distorted to the nearest asymmetric twist (for **1**) or asymmetric envelope (for **2**) along the pseudo-rotation pathway.

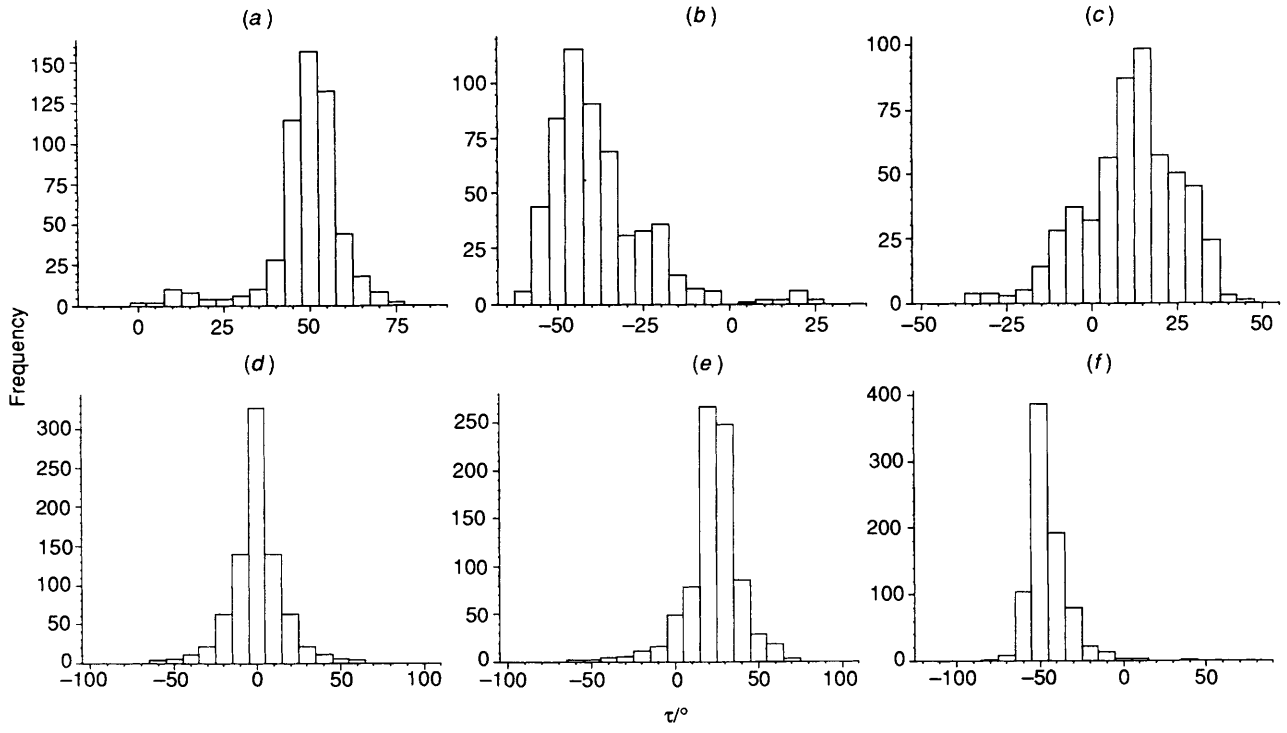

Fig. 7 Histograms of the unique intra-ring torsion angles (τ_{1-3}) within the clusters of conformations observed in Figs. 1 and 2: (*a*)–(*c*) show τ_{1-3} for the M(dppe) structures with $-90 \leqslant \varphi \leqslant 90°$; (*d*)–(*f*) show τ_{1-3} for the M_2(μ-dppm) structures with $180 \leqslant \varphi \leqslant 360°$

Table 2 Statistics for ring torsion angles (°)

	M_2(μ-dppm)($180 < \varphi < 360°$)		M(dppe)($-90 < \varphi < 90°$)	
Torsion angle	Mean	Standard deviation	Mean	Standard deviation
τ_1	0.0	15.71	48.75	11.02
τ_2	22.93	16.24	−37.82	14.26
τ_3	−44.84	12.13	11.35	14.27
τ_4	44.84	12.13	11.35	14.27
τ_5	−22.93	16.24	−37.82	14.26

Analysis of the M_2(μ-dppm) distribution also suggests that the envelope is more rigidly adopted for longer metal–metal distances. Fig. 6 shows a scatterplot of metal–metal separation against φ for those data in the unique region of conformation space, $0 \leqslant \varphi \leqslant 90°$. The spread of points implies that for longer metal–metal distances the phase angles φ are closer to 90° (or 270°) than for shorter metal–metal distances, where a wider spread of φ is seen.

It has been shown that for ethylenediamine and 1,2-bis(diphosphino)ethane chelate five-membered rings the ethylene C–C bond often is the least variable of the five ring torsion angles.[9] In the present study of M(dppe) chelate rings the distributions of torsion angles τ_{1-5} are consistent with these previous findings. Fig. 7(*a*)–(*c*) and Table 2 show the distribution of τ_{1-5} for conformations of the δ form, in which τ_1 is positive (*i.e.* within the restriction $-90 < \varphi < 90°$). It is clear that τ_1 tends to have the largest values of all five of the intra-ring torsion angle distributions in the δ form, with the least spread in values. Hall *et al.*[9] suggested there to be little energy difference between the conformations with $\varphi = 0$ or $\pm 18°$. The argument is that the C–C torsion angle, τ_1, is relatively unaffected on changing φ through this range, hence some distortion of phase angle is possible without unfavourable increase in energy, because the torsional energy of the ring is most strongly dependent on τ_1. This is consistent with the observed spread for dppe conformations about the $\varphi = 0$, 180°, C_2 twist forms discussed above. Fig. 7(*d*)–(*f*) illustrate the corresponding distributions for the M_2(μ-dppm) fragments within the restriction that $180 < \varphi < 360°$, *i.e.* for one of the two separate clusters of points in Fig. 1. In this case it is the M–P–C–P torsion angles, τ_3 (and by symmetry τ_4), which are the most restricted (and the furthest from zero) of the intra-ring torsion angles. The distribution of torsion angle τ_1 is symmetrical about zero, the value required by the envelope conformation of these M_2(μ-dppm) species.

In Fig. 8(*a*) and (*b*) the chelate rings of ten prophos and six chiraphos complexes taken from the CSD have been superimposed by least-squares fit. The conformations fall in the range between the C_2 twist and either adjacent asymmetric envelope conformation, *i.e.* $-18 < \varphi < 18°$. As a consequence of the substituents on the ethylene carbons, the conformations are forced to be close to one of the two twist forms, in order to keep the methyl groups in equatorial sites on the five-membered ring. These conformations are flexible to a degree, but the other twist conformation is of course at higher energy having axial sites occupied by methyl groups. This twist is the source of chirality for the enantioselective catalytic behaviour exhibited by complexes of such diphosphines. A corresponding disturbance of the population of conformation space may be achieved for M_2(μ-dppm) derivatives by replacing one of the CH_2 hydrogens by, *e.g.*, a methyl group, thereby locking the five-membered conformation into one of the two envelope forms, in practice the one which places the bulky substituent in the less-congested equatorial site.

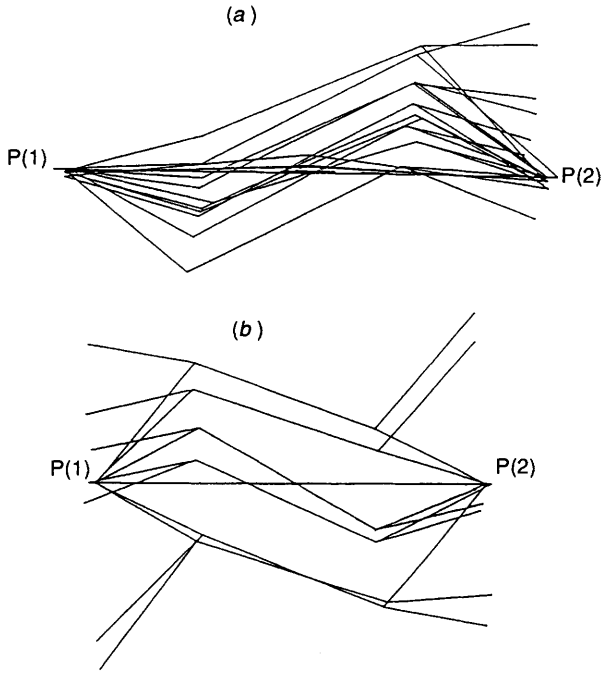

Fig. 8 Superposition of geometries of (*a*) ten prophos chelate rings and (*b*) six chiraphos chelate rings, present in metal complexes

Pseudo-rotation Pathway.—Taking the view of Dunitz and Bürgi,[25] that reaction pathways may be identified from the geometries of (sub)molecular fragments observed in the solid state, Murray-Rust and Motherwell[18] have shown how crystal data may be used to map the low-energy preferred conformations on a restricted pseudo-rotational pathway in the five-membered rings of furanoside derivatives. The scatterplots of Figs. 1 and 2 show clearly defined pathways between the preferred, more densely populated regions of conformation. It is notable that all the observed geometries for both fragments **1** and **2** are on paths which lie far from the plot origin. Thus there are no structures at all with planar five-membered rings, which conformation would correspond to the origin of these plots. In the Murray-Rust and Motherwell study relatively tight clustering of the data points was observed, close to the preferred twist conformations. In contrast in our study, especially for the M(dppe) fragment, wide spreads of points are observed, which appear to map almost the entire pseudo-rotation pathway. Dunitz and Bürgi[26] have pointed out the hazards of making a direct analogy between the population of a parameter space plot for a fragment (such as Figs. 1 and 2) and the potential-energy hypersurface for reactions of the fragment. Bearing in mind these reservations, certain qualitative conclusions can nevertheless be drawn from the appearance of Figs. 1 and 2. The well defined distribution of conformations indicates that ring inversion for both **1** and **2** would be expected to occur by a pseudo-rotation pathway rather than a mechanism involving a planar intermediate. This is indicated by the absence of any points in the p.c. score (and AS) scatterplots close to the origin of the plots, as noted above. Secondly the transition state for ring inversion is likely to be the twist conformer for **1** and the envelope conformer for **2**, respectively. Finally, and less definitively, the barrier to inversion of M_2(μ-dppm) rings is likely to be higher than that for M(dppm) rings in the light of the relative scarcity of points close to the putative transition state for **1**.

Phenyl-group Conformations.—The conformations of the four phenyl groups in each of fragments **1** and **2** were studied in terms of the torsion angles ω_{1-4}. The relationships between these four parameters were examined using scatterplots where appropriate. For each fragment studied the C_{2v} symmetry of the frame group allows four isometric sets of parameters (as defined above) to describe five-membered ring conformations. These four represent the conformation in each unique quadrant of φ (*i.e.* 0–90, 90–180, 180–270, 270–0°). In the scatterplots below used for the analysis of the phenyl group conformations, torsion angles for each fragment are generated for one half of this fully symmetry expanded data set. For each of **1** and **2** the half selected was chosen to contain only one of the two virtually isolated clusters of five-membered ring conformations as shown above. Fragments with $180 \leqslant \varphi \leqslant 360°$ for M_2(μ-dppm), and $-90 \leqslant \varphi \leqslant 90°$ for M(dppe), were employed in this part of the study. The scatterplots cover regions of conformational space for all points within the ranges of ω from −180 to +180° applying the local C_2 symmetry of each phenyl group (*i.e.* the 180° periodicity of ω_i). Therefore the scatterplots contain 8 × 409 points for M_2(μ-dppm) and 8 × 274 points for M(dppe) fragments respectively.

Our objective is to identify the preferred conformations of the phenyl groups and examine how they are related to the five-membered ring conformations. The preferred phenyl group conformations may be identified from scatterplots, and they and the pathways between them described using similar terms to those applied to previous studies of correlated motion in aryl propellers[11] in terms of ring 'flip' mechanisms. A flip is defined as occurring when the plane of the aryl ring becomes perpendicular to the plane of the C_{ipso}–P–C_{ipso} unit for that diaryl fragment, during aryl ring rotation about the P–C_{ipso} bond. This is illustrated for phenyl X, where the plane of X is perpendicular to the plane of the paper containing the C_{ipso}–P–C_{ipso} unit.

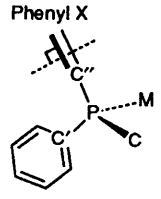

In M_2(μ-dppm) *fragments.* As described above, the conformations of the five-membered ring of fragment **1** are observed to concentrate near $\varphi = 90$ and 270°, in an envelope conformation. Consequently for the portion of the data used in this part of the study ($\varphi = 270 \pm 90°$) phenyl groups A and D are found in essentially axial positions while B and C are in more equatorial sites (see Fig. 5). Furthermore given that the scatterplots of ω_i below contain two symmetry-equivalent conformations there is a two-fold degeneracy of phenyl groups within this data set. Thus for every fragment with some orientation of phenyl A (ω_1) there is an equivalent fragment with the mirror image conformation at ring D (with ω_4 for this fragment = 180 − ω_1 for the first fragment) and similar pairing of ω values for rings B and C. This leads to mirror symmetry of plots of ω_1 *vs.* ω_4 and ω_2 *vs.* ω_3 and the equivalence of a plot of ω_1 *vs.* ω_3 with that for ω_2 *vs.* ω_4 (and of ω_1 *vs.* ω_2 with that for ω_3 *vs.* ω_4).

The scatterplot in Fig. 9 illustrates the conformations of phenyl groups on the same phosphorus (*i.e.* ω_1 is plotted against ω_2). The main area of point concentrations is in the regions **Z**, which represent a one-ring-flip conformation. These regions are connected by more thinly populated regions which slope from high ω_1 and low ω_2 to low ω_1 and high ω_2 (*i.e.* in which ω_1 and ω_2 are negatively correlated, approximately following a line of equation $\omega_1 = 70 - \omega_2°$). These regions are further connected by small regions in which ω_1 and ω_2 are positively correlated. This pattern of populated regions may be interpreted in terms of the possible mechanisms of coupled phenyl group rotation. Fig. 9 also illustrates the favoured processes, the one-ring-flip path linking the clusters of points **Z** along the line of negative slope and the short, two-ring-flip, path linking these lines. On the one-ring-flips pathway the phenyl groups perform a geared disrotatory motion, rotating in the opposite sense to maintain a dihedral angle of approximately 90° between their planes.

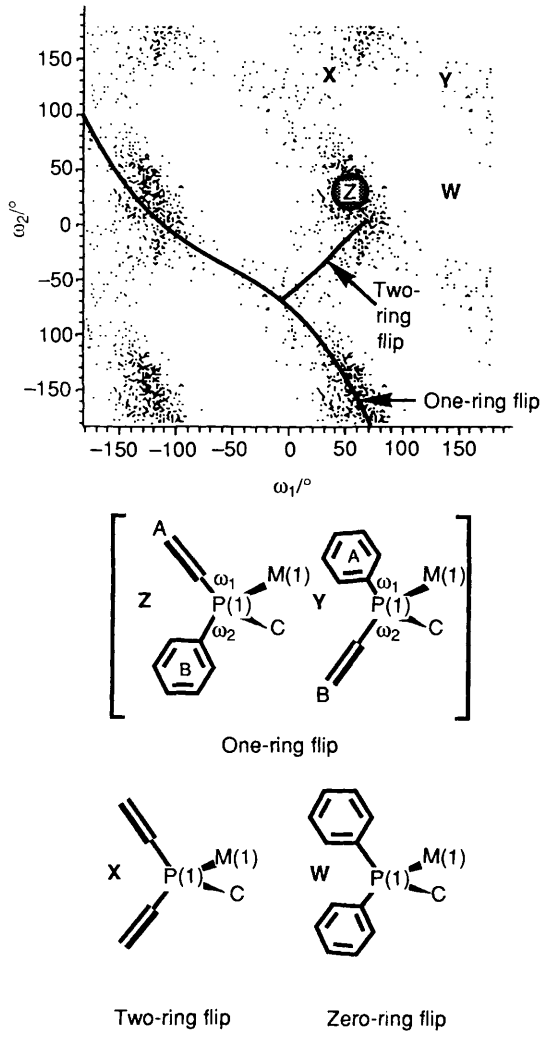

Fig. 9 Torsion angle plot for two phenyls on the same phosphorus (*i.e.* A and B) for $M_2(\mu\text{-dppm})$ structures with $180 \leqslant \varphi \leqslant 360°$. Illustrations of conformations **W**, **X**, **Y** and **Z**. Two phenyl ring rotation pathways are illustrated by the solid lines

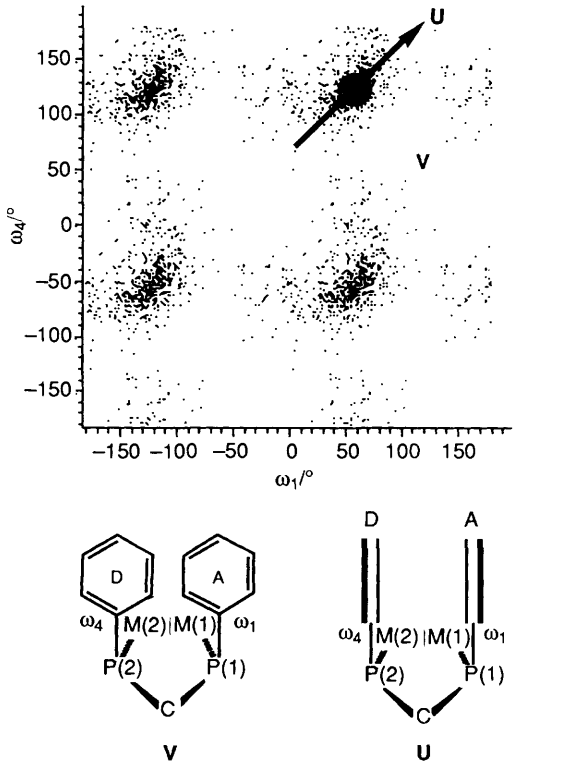

Fig. 10 Torsion angle plot for phenyls groups A and D for $M_2(\mu\text{-dppm})$ structures with $180 \leqslant \varphi \leqslant 360°$. Illustrations of conformations **U** and **V**. The arrow represents the positive correlation between ω_1 and ω_4 within the cluster of points at **U**

Kaftory *et al.*[11c] indicate in their diaryl system that a second one-ring-flip conformation is as likely as the first. However, here a lower population is seen at **Y** in comparison to **Z**, corresponding to the second one-ring flip. The tendency for low population at **Y** and less spread in ω_1 is due to the rotation of phenyl A being restricted in its predominantly axial location (see below).

Evidence for the second rotation mechanism, *via* the two-ring-flip intermediate, **X**, is clearly present in Fig. 9. The positive slope of the points in the vicinity of **X** indicates that this is a conrotatory process where the phenyl groups rotate in the same sense which occurs only when both the phenyl groups are close to the flip position. Kaftory *et al.*[11c] suggest that in their system that this pathway is higher in energy than the one-ring flip. There appears to be no strong distinction between the one- and two-ring flip mechanisms in this data set as indicated by the density of points on the two paths. A third possible mechanism for coupled phenyl group rotation is *via* the zero-ring-flip intermediate whose position is shown at **W**. This region is totally clear of points on Fig. 9, reflecting the high-energy, mutually edge-on conformations of rings A and B for such an intermediate.

Fig. 10 shows the scatter plot for ω_1 *vs.* ω_4, illustrating the conformations of phenyl groups A and D which are on phosphorus atoms P(1) and P(2) respectively. Phenyl groups A and D are both in axial sites for five-membered ring conformations close to $\varphi = 90°$ (see Figs. 5 and 10). The phenyl group conformations may be seen to cluster tightly in a region centred on the midpoint of arrow **U**, with the spread of points in the clusters following a positive gradient. This indicates considerable restriction and coupling of the rotation of rings A and D (ω_1 and ω_4 respectively), as they clash across the dppm bridge in conformations where they are 'face on' as in conformation **V**. A conrotatory motion of the two rings is indicated by the positive gradient of the cluster **U**, where the rings may twist from the conformation **U** but must remain approximately parallel to one another. The pathway connecting conformations **U** may be tentatively identified as being with the sparsely populated regions running parallel to the axes between the clusters of points in Fig. 10. Such pathways correspond to one phenyl group (A for the vertical path, D for the horizontal) remaining essentially stationary in the edge-on conformation of **U**, while the other rotates through the face-on conformation of **V** and eventually reaches a second edge-on orientation.

Fig. 11 shows the scatterplot for ω_1 *vs.* ω_3, illustrating the conformations of phenyl groups A and C which are on phosphorus atoms P(1) and P(2) respectively. The clustering at region **T** may be seen as a consequence of combating the effects of the diaryl gearing seen in the ω_1 *vs.* ω_4 and ω_1 *vs.* ω_2 plots (and hence also for ω_3 *vs.* ω_4), to give a preferred conformation **T**. The implication of Fig. 10 is that ω_1 and ω_4 are the most restricted torsion angles, as a result of the mutual proximity of phenyls A and D. The diaryl gearing of rings C and D ensures a transmission of steric effects out to the conformation of phenyl C, as represented by ω_3.

Fig. 12 shows the scatter plot for ω_2 *vs.* ω_3, illustrating the conformations of phenyl groups B and C which are on phosphorus atoms P(1) and P(2) respectively. Being in equatorial sites these phenyl groups are generally much further apart than A and D, so less direct cross-ring influence is found. However, some clustering centred at region **R** indicates that the gearing around the ring *via* the interaction of phenyls A and D results in a weak correlation where the conformation **R**

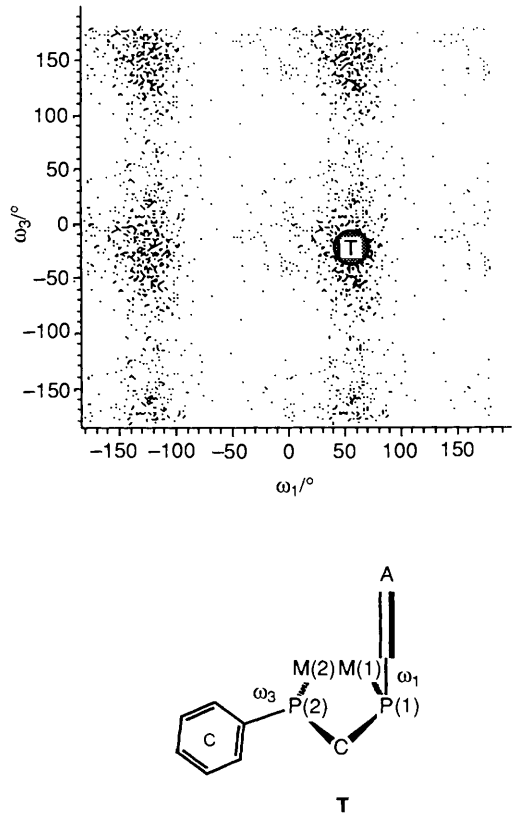

Fig. 11 Torsion angle plot for phenyls groups A and C for $M_2(\mu$-dppm) structures with $180 \leqslant \varphi \leqslant 360°$. Illustration of conformation **T**

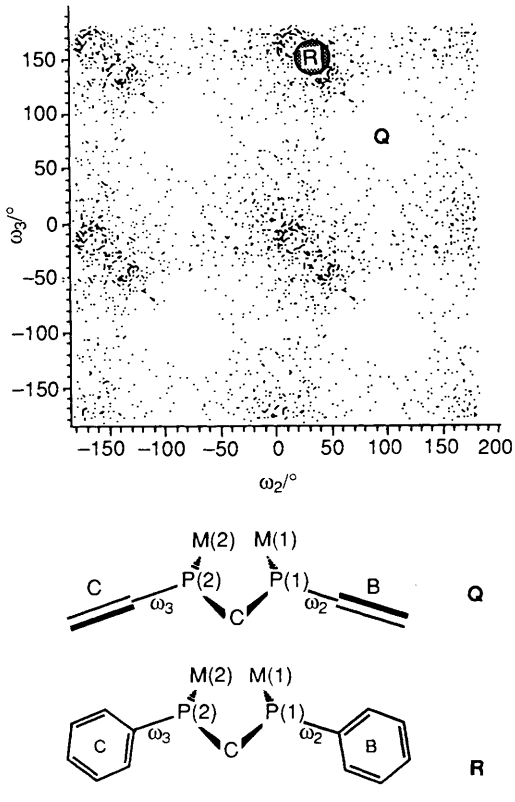

Fig. 12 Torsion angle plot for phenyls groups B and C for $M_2(\mu$-dppm) structures with $180 \leqslant \varphi \leqslant 360°$. Illustration of conformations **Q** and **R**

is the most densely populated centre, and conformation **Q** has zero population density.

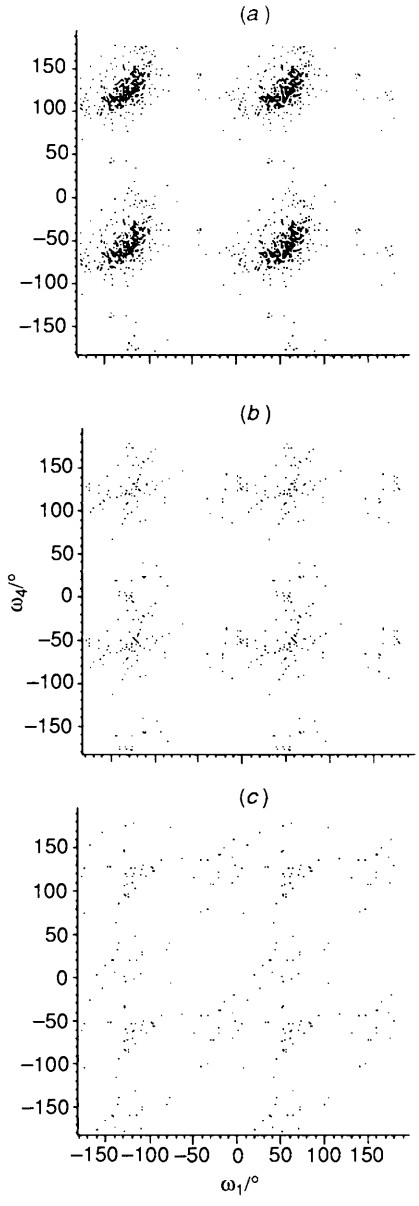

Fig. 13 Torsion angle plots for phenyls groups A and D for $M_2(\mu$-dppm) structures (see also Fig. 12) for selected regions of φ: (*a*) 252–288; (*b*) 234–252 and 288–306°; (*c*) 180–234 and 306–360°

The conformation of the M_2P_2C ring can vary away from a pure envelope, as seen above. As deviation from $\varphi = 270°$ occurs, phenyls A and D will vary from axial positions. Consequently ω_1 and ω_4 may experience variation in the restrictions of the values they may take. Fig. 13(*a*)–(*c*) illustrates this behaviour by showing the ω_1 *vs.* ω_4 scatterplot (see Fig. 10) for selected regions of φ: (*a*) 252–288; (*b*) 234–252 and 288–306; (*c*) 180–234 and 306–360°. The ω distributions are tightly concentrated for φ near 270°, and more spread for φ approaching 180 and 360°, as the conformation of the five-membered ring deviates from a C_s envelope towards a C_2 twist, allowing the phenyl groups A and D to move apart. As a consequence the clustering of points and hence the conformational preference for these two phenyl groups almost disappears in Fig. 13(*c*), indicating that the cross $M_2(\mu$-dppm) ring influence is greatly reduced as a more twisted conformation develops. The implication is that in order to allow rotation of the axial phenyl groups the five-membered ring conformation would distort away from the envelope to a twist and then relax back to envelope after phenyl rotation had taken place.

In M(dppe) *fragments.* The analysis of five-membered

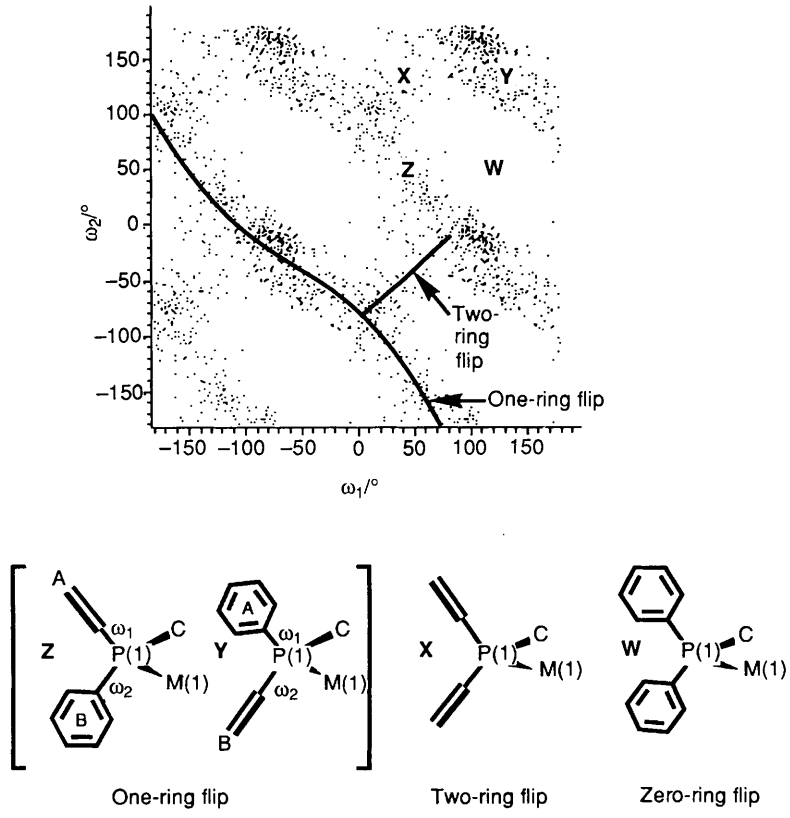

Fig. 14 Torsion angle plot for two phenyls on the same phosphorus (*i.e.* A and B) for M(dppe) structures with $-90 \leqslant \varphi \leqslant 90°$. Illustrations of conformations **W**, **X**, **Y** and **Z**. Two phenyl ring rotation pathways are illustrated by the solid lines

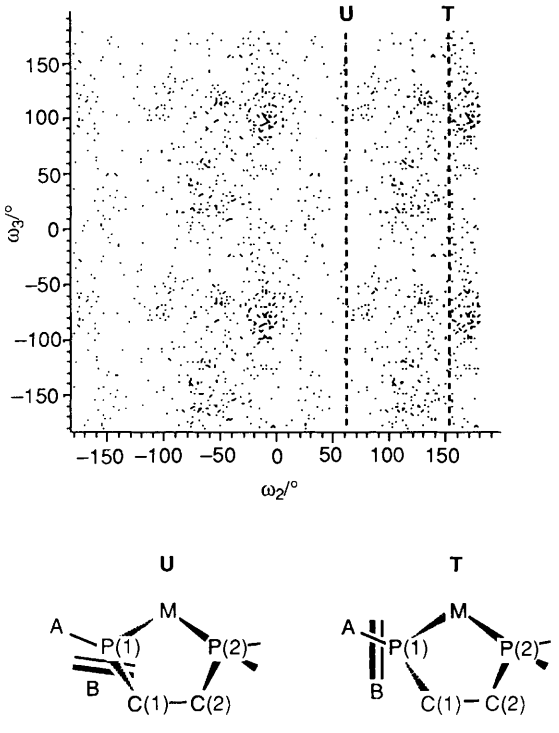

Fig. 15 Torsion angle plot for phenyls groups B and C for M(dppe) structures with $-90 \leqslant \varphi \leqslant 90°$. Illustrations of conformations **U** and **T**

M(dppe) chelate rings above indicates that a C_2 twist form is the predominantly adopted conformation. As shown in Fig. 5 this tends to create pseudo-axial and pseudo-equatorial sites for the phenyl groups, resulting from the generally large C–C torsion angle τ_1, of the chelate ring. The conformations studied here are restricted to the δ form where $\varphi = 270°$ (or $-90°$) through 0 to 90°. As discussed above for the M_2(μ-dppm) case this choice leads to a two-fold degeneracy of the ω scatterplots below. In this case, however, for every fragment with some orientation of phenyl A (ω_1) there is an equivalent fragment with the same conformation at ring C (with ω_3 for this fragment = ω_1 for the first fragment) and similar pairing of ω values for rings B and D. This leads to mirror symmetry of plots of ω_1 *vs.* ω_3 and ω_2 *vs.* ω_4 and the equivalence of a plot of ω_1 *vs.* ω_2 with that for ω_3 *vs.* ω_4 (and of ω_1 *vs.* ω_4 with that for ω_2 *vs.* ω_3).

The scatterplot of Fig. 14 shows the conformations of phenyl groups on the same phosphorus (*i.e.* ω_1 *vs.* ω_2). In comparison to the situation for M_2(μ-dppm) fragments (see Fig. 9) the M(dppe) fragments show less-marked preferences between conformers **X**, **Y** and **Z**. Fig. 14 shows the interconversion pathways linking these conformations, the negatively sloping disrotatory one-ring-flip path, or the positively sloping conrotatory two-ring flip [*cf.* Fig. 9 for M_2(μ-dppm)]. The implications of these plots are that the two one-ring-flip conformers (**Y** and **Z**) are closer in energy and that the one- and two-ring flip pathways for phenyl group rotation are approximately equally energetically viable. As before the region corresponding to the zero-ring-flip conformation **W** is not populated at all, as above, because of the steric interference of the two rings A and B. This pattern is therefore closer than that for fragment **1**, to that seen for the $R'_2C{=}CR_2$ (R′ = aryl, R = any substituent) system.[11c]

Fig. 15 shows the conformations of phenyl groups on different phosphorus atoms in M(dppe) fragments, in this case phenyls B and C (and hence A and D also) as a scatterplot of ω_2 *vs.* ω_3 (*cf.* Fig. 10 for fragment **1**). In contrast to the M_2(μ-dppm) case there is no pronounced clustering of points in Fig. 15. Instead rather weak restrictions on values of ω_2 (and hence ω_4 also) can be seen, resulting in vertical bands of higher (**T**) and lower (**U**) population. The bands of denser population **T** represent the 'edge' conformation of phenyls B (and D) and the spread of ω_3 values implies virtually free rotation of phenyl group C (and A).

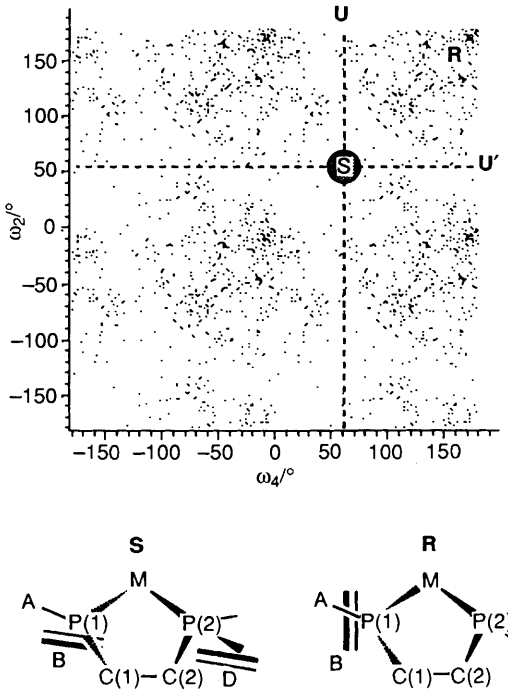

Fig. 16 Torsion angle plot for phenyls groups B and D for M(dppe) structures with $-90 \leqslant \varphi \leqslant 90°$. Illustrations of conformations **S** and **R**

The bands of lower density **U** correspond to disfavoured face-on conformations of the pseudo-axial phenyls B and D. These conformations bring the *ortho*-hydrogens into the proximity of the pseudo-axial hydrogen on carbons of the ethylene link C(1)–C(2) (see below and Fig. 15) and eclipse the *ipso*-carbon of the other (pseudo-equatorial) phenyl ring attached to the phosphorus.

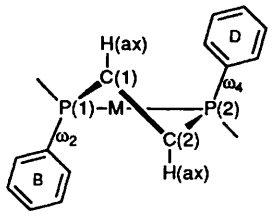

Fig. 16 shows the conformations of phenyl groups B and D in the form of a scatterplot of ω_2 *vs.* ω_4. The pattern observed displays the combination of restrictions on values of ω_2 and ω_4 which were discussed above. Consequently, a distinct unpopulated horizontal band marked **U**′ and a low populated vertical band marked **U** reflect the preferences of phenyls B and D respectively to avoid 'face-on' conformations. Understandably, given the pseudo-axial positions of both phenyls B and D, these groups show a preference for conformation **R** where both rings are 'edge on', and low population at **S** where both rings are 'face on'. Fig. 17, which illustrates the conformations of phenyl groups A and C as a scatterplot of ω_1 *vs.* ω_3, has a less-evident pattern than Fig. 16. Although no highly favoured or disallowed regions are seen, the highest concentration of points is at region **P**. This conformation may be seen as a consequence of the relationship between phenyls on the same phosphorus, where a 90° phase difference results (see Fig. 14), and the relationship between phenyls B and D. If an 'edge on' disposition is favoured by phenyls B and D, then the 90° phase relationship of A and C respectively will tend to impose a preference of 'face-on' orientation to A and C.

The patterns of phenyl ring conformational behaviour are obviously much less clear for M(dppe) than for $M_2(\mu\text{-dppm})$ fragments. An improved picture can be achieved by restricting

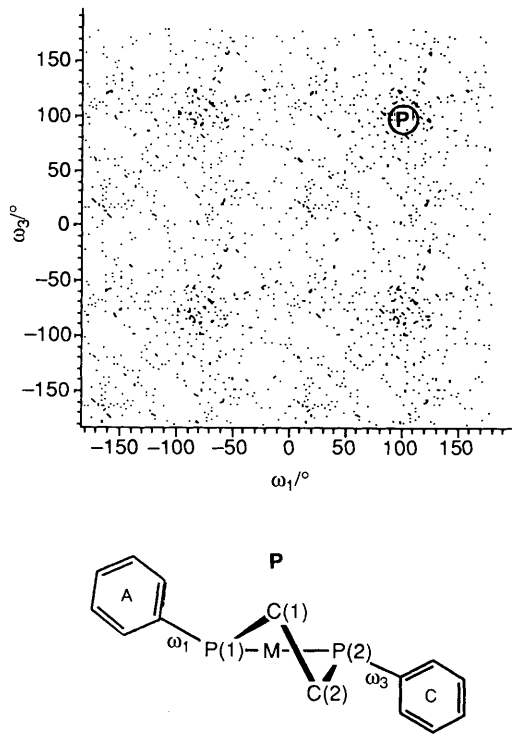

Fig. 17 Torsion angle plot for phenyls groups A and C for M(dppe) structures with $-90 \leqslant \varphi \leqslant 90°$. Illustration of conformation **P**

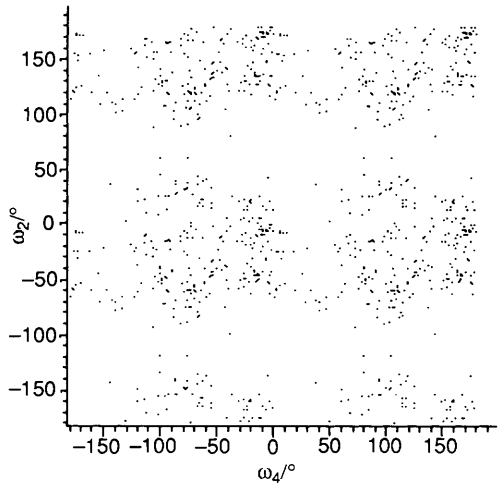

Fig. 18 Torsion angle plot for phenyls groups B and D for M(dppe) structures with $0 \leqslant \varphi \leqslant 90°$ (*cf.* Fig. 19)

the analysis to one quadrant of φ, *i.e.* to a unique portion of the conformation space. The majority of δ-form M(dppe) fragments exist with conformations of φ near 0°, so in this portion of conformation space phenyl D is primarily pseudo-axial. However the M(dppe) chelate ring conformations are quite variable (see above), and as φ increases D becomes more axial in character to a maximum at $\varphi = 90°$. Phenyl B is also pseudo-axial at $\varphi = 0°$ but in contrast becomes more equatorial as φ increases towards 90° which distinguishes it from phenyl D. Similarly phenyl groups A and C are uniquely distinguishable, as shown in Fig. 5. Therefore, for a particular fragment, each of the four ω values represents a phenyl group in a specifically defined environment. The phenyl groups will be expected to experience differing conformational restrictions in these sites, and their orientations are likely to depend on the conformation of the five-membered ring.

Fig. 18 shows a scatterplot of ω_2 *vs.* ω_4 for this unique portion

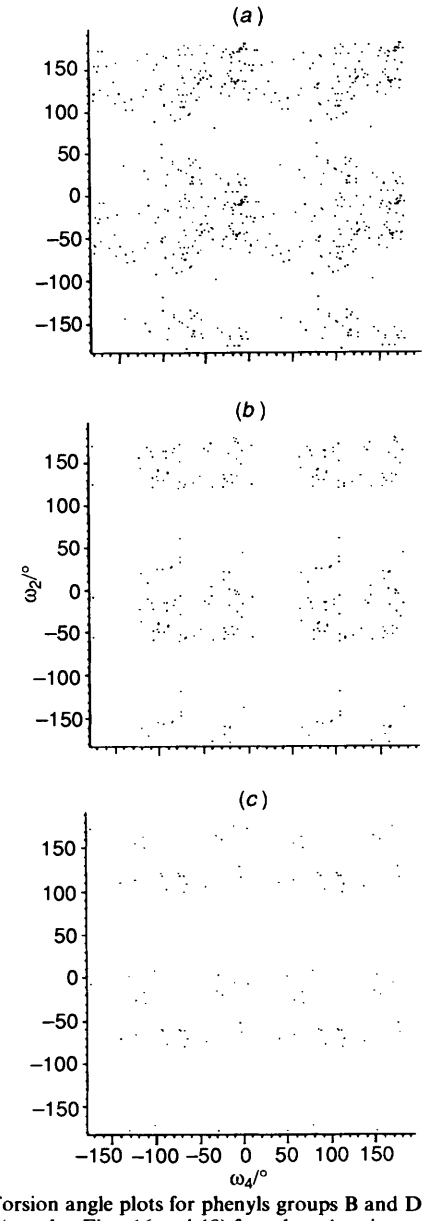

Fig. 19 Torsion angle plots for phenyls groups B and D for M(dppe) structures (see also Figs. 16 and 18) for selected regions of φ: (*a*) 0–18; (*b*) 18–36; (*c*) 36–90°

of φ space, and shows a loss of the mirror symmetry as compared with Fig. 16. It can be seen that ω_2 is the most strongly restricted torsion angle of the M(dppe) system. In Fig. 18 there is less apparent restriction on ω_4 than on ω_2, which results in more evident horizontal bands of low population than vertical bands of low population. The causes of restrictions on the pseudo-axial phenyls B and D have already been considered above and may differ from each other here as the former becomes more 'axial' while the latter becomes more 'equatorial' on changing φ from 0 to 90° (see Fig. 5).

The distribution of ω_2 *vs.* ω_4 is examined as a function of φ between 0 and 90° in Fig. 19(*a*)–(*c*). As φ increases, phenyl D moves from pseudo-axial into a more equatorial position, whereas phenyl B moves from pseudo-axial into a more axial position. As can be seen in Fig. 19(*a*)–(*c*) in which the sections move to larger φ, from 0–18, to 18–36, to 36–90°, respectively, the exclusion area for ω_2 widens as the restriction on the orientation on ring B increases as it becomes more axial.

Discussion

The use of p.c.a. and inspection of scatterplots and histograms of torsion angles and principal components has allowed identification of the favoured conformations of the five-membered rings and their attached phenyl groups in the topically equivalent systems **1** and **2**. For the M_2(μ-dppm) fragment the preferred conformation of the M_2P_2C five-membered ring is the C_s envelope. In contrast, for the M(dppe) fragment the C_2 twist conformation is preferred. The difference between these two systems extends to the flexibility or range of conformations observed, with the M(dppe) fragment apparently being the more flexible of the two. These two observations may be rationalised by viewing the M_2P_2C unit within the M_2(μ-dppm) fragment as having conformational preferences more akin to five atoms of a cyclohexane ring than to those of a cyclopentane ring. Thus the M • • • M separations (2.5–3.5 Å) are much closer to the 1,3-C • • • C distances in cyclohexanes (*ca.* 2.5 Å) than the 1,2-C–C distances in cyclopentanes (*ca.* 1.5 Å). As a consequence the conformations adopted by the M_2P_2C unit are essentially portions of chair (for the typical C_s conformations) or twist-boat (for those deviating from the C_s geometry) conformations familiar from the conformational analysis of cyclohexanes. As further evidence of this analogy, the preference for the envelope (semi-chair) conformation with φ close to ±90° becomes more and more pronounced as the M • • • M distance increases (see Fig. 6). In contrast for the M(dppe) fragment the analogy with the classical conformational analysis for cyclopentane and heterocyclopentanes is more appropriate. In *both* systems, however, clear evidence of the pseudo-rotation pathway for ring inversion is seen in the p.c. score (and Altona–Sundaralingam) scatterplots.

In each system the symmetry of their conformation space (isomorphic with C_{2v}) is such that the observed five-membered ring conformations cluster around two points (corresponding to conformations of C_s and C_2 symmetry for **1** and **2** respectively) related by mirror symmetry and apparently corresponding to minima in the potential-energy hypersurface. The possibility of restricting the possible conformations to only one of these energy minima by appropriate substitution of the ring carbon atom(s) is one that has been achieved, notably in the syntheses and exploitation of *S,S*-chiraphos and *R*-prophos.

For both systems the clearest conformational patterns for the phenyl group orientations occurs within the PPh_2 units. In each case there is substantial population of conformations corresponding to both one- and two-ring flip pathways for phenyl ring rotation about the P–C_{ipso} bonds. The transmission of conformational information from one phosphorus to another, across the five-membered ring, is much more effective in the case of the M_2(μ-dppm) system. This is a consequence of two phenyl rings being forced into 1,3-axial sites in which they interact strongly; the presence of such sites is itself a consequence of the preference of the M_2P_2C ring for an envelope conformation. In addition there is evidence (Fig. 13) to suggest that the flexibility of this ring (and deviation of its conformation from the envelope towards a C_2 geometry) is itself a prerequisite for the complete rotation of these phenyl groups. In the absence of such flexibility the axial phenyls cannot get past one another and their rotational motion is restricted to a coupled wagging. Finally the coupling of phenyl ring rotations within PPh_2 units noted above implies that there will be (as is observed) a general coupling of phenyl group orientations throughout the M_2(μ-dppm) system.

The situation in the M(dppe) system is rather different. Although coupling of phenyl ring orientations within PPh_2 units is clearly observed (Fig. 14) there is only very weak transmission of orientational information from the phenyls of one phosphorus to those of the other and the very diffuse patterns observed in Figs. 15–19 result. This is a consequence of two related phenomena. First, the phenyl rings on the two phosphorus atoms are held in sites in which there is relatively little transannular clashing of phenyls, as is illustrated in Fig. 5. Secondly the MP_2C_2 five-membered ring itself is highly flexible and permits a disposition of phenyl groups appropriate to near-

free rotation of the phenyls. It seems (as deduced from Fig. 19) that the conformational options for the phenyl groups do become more limited when the MP_2C_2 ring adopts conformations away from the C_2 twist geometry. Such control of phenyl group orientations that does occur appears to result from interactions between the *ortho*-hydrogens of the pseudo-axial phenyl groups and the axial hydrogens of the ring carbons. This results in a weak preference for 'edge-on' conformations of these phenyls.

For both systems it is clear that there is a correlation between the conformation adopted by the five-membered ring and the tenable orientations of the attached phenyl groups. The greater rigidity and preference for the envelope conformation forces greatly restricted and highly coupled orientations on the phenyls of the M_2(μ-dppm) system while there is much less constraint on those of the M(dppe) fragment.

In summary the M_2(μ-dppm) unit tends to adopt a conformation indicated below (and its mirror image) albeit with

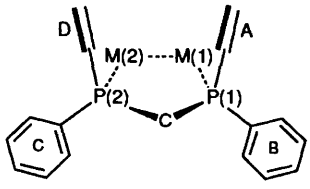

significant flexibility. In contrast the M(dppe) fragment has a *very* weak preference to adopt the conformation illustrated below and wide variations are seen especially in the phenyl group orientations (*cf.* similar conclusions drawn for chiral dppe derivatives[27]), which seem likely to undergo near-free but coupled rotation in the absence of axial substitution on the ring carbons or coupled rotation in the absence of axial substitution on the ring carbons or *ortho* substitution on the phenyls.

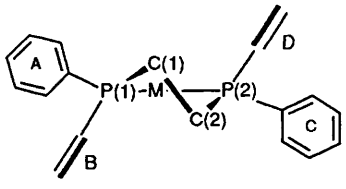

These observations allow some insight into the design of ligand systems for efficient induction of asymmetric chemistry at the metal atom(s). Thus for dppe derivatives one would suggest: (1) the use of bulky substituents, or possibly better still, fusing of the five-membered ring with a six-membered ring so as to lock the ring conformation adopted into one of the two (δ or λ) favoured for M(dppe) species; and (2) the *additional* substitution of one or both of the remaining (axial) sites on the ring carbons with *e.g.* methyl groups, in order to restrict the orientational variability of the phenyl groups. While suggestion (1) is not new and has been realised, (2) is we believe one worthy of the attention of synthetic chemists. On a cautionary note, it has been pointed out[28] that flexibility of ligands such as these is important to their successful function as part of catalytic species. Furthermore it is not always the favoured diastereomer of the ligand–metal–substrate complex which leads to the observed chiral product.[29] However it remains likely that a system allowing less flexibility in its conformations will express chirality more effectively than a more flexible analogue. More quantitative attempts at design of metal–ligand ensembles for (chiral) synthetic applications will have to await the further development of mathematical modelling procedures for the study of transition-metal complexes such as those studied here. In any event the data presented will permit calibration of such modelling procedures, since they should give semiquantitative agreement with the conformational preferences we have observed.

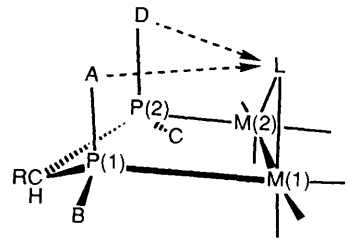

$\phi = 270°$

Fig. 20 Non-bonded interactions providing an asymmetric environment for ligand L in M_2(μ-dppm) complexes substituted at the dppm methylene carbon

In contrast to the situation for dppe complexes the conformational preferences of the M_2(μ-dppm) complexes are such that there is every reason to expect that derivatives (*e.g.* having a methyl substituent at the methylene carbon) of this unit would be able to exert control of the chemistry at the dimetal centre when that chemistry occurs in a site *cis* to the two M–P bonds, as illustrated in Fig. 20.

The techniques applied here (symmetry expansion to fill conformation space and principal component analysis) have permitted a satisfactory separation of the important aspects of conformational variability. This has allowed a conformational analysis of a much larger data set than has previously been attempted for diphosphine or related systems. In future papers we will demonstrate that this approach is a powerful one for the study of more complex conformational problems.

Acknowledgements

We thank the many chemists and crystallographers who synthesised and determined the structures of the molecules listed. We thank the SERC for a studentship (to D. A. V. M.).

References

1 Part 3, B. J. Dunne, R. B. Morris and A. G. Orpen, *J. Chem. Soc., Dalton Trans.*, 1991, 653.
2 C. A. McAuliffe and W. Levason, *Phosphine, Arsine and Stibine Complexes of the Transition Metals*, Elsevier, Amsterdam, 1979.
3 E. C. Alyea and D. Meek (Editors), *Adv. Chem. Ser.*, 1982, **196**; *Homogeneous Catalysis with Metal Phosphine Complexes*, ed. L. H. Pignolet, Plenum, New York, 1983.
4 R. J. Puddephatt, *Chem. Soc. Rev.*, 1983, **12**, 99; B. Chaudret, B. Delavaux and R. Poilblanc, *Coord. Chem. Rev.*, 1988, **86**, 191.
5 D. M. A. Minahan, W. E. Hill and C. A. McAuliffe, *Coord. Chem. Rev.*, 1984, **55**, 3; W. Levason and C. A. McAuliffe, *Adv. Inorg. Chem. Radiochem.*, 1972, **14**, 173; C. A. McAuliffe, in *Comprehensive Coordination Chemistry*, eds. G. Wilkinson, J. A. McCleverty and R. D. Gillard, Pergamon, Oxford, 1987, vol. 2, p. 989.
6 M. D. Fryzuk and B. Bosnich, *J. Am. Chem. Soc.*, 1977, **99**, 6262.
7 M. D. Fryzuk and B. Bosnich, *J. Am. Chem. Soc.*, 1978, **100**, 5491; B. Bosnich and M. D. Fryzuk, *J. Am. Chem. Soc.*, 1979, **101**, 3043.
8 J. E. Kilpatrick, K. S. Pitzer and R. Spitzer, *J. Am. Chem. Soc.*, 1947, **69**, 2483; J. B. Hendrickson, *J. Am. Chem. Soc.*, 1961, **83**, 4537; S. Lifson and A. Warshel, *J. Chem. Phys.*, 1969, **49**, 5116.
9 E. J. Corey and J. C. Bailar, jun., *J. Am. Chem. Soc.*, 1959, **81**, 2620; J. K. Beattie, *Acc. Chem. Res.*, 1971, **4**, 253; The Commission on the Nomenclature of Inorganic Chemistry of the International Union of Pure and Applied Chemistry, *Inorg. Chem.*, 1970, **9**, 1; F. Pavelcik and E. Luptakova, *Collect. Czech. Chem. Commun.*, 1990, **55**, 1427, 312; J. R. Gollogly and C. J. Hawkins, *Inorg. Chem.*, 1969, **8**, 1168; L. Battaglia, D. Delledonne, M. Nardelli, C. Pelizzi, G. Predieri and G. P. Chiusoli, *J. Organomet. Chem.*, 1987, **330**, 101; M. C. Hall, B. T. Kilbourn and K. A. Taylor, *J. Chem. Soc. A*, 1970, 2539.
10 D. Cremer, *J. Chem. Phys.*, 1979, **70**, 1898; 1978, **69**, 4456; D. Cremer and J. A. Pople, *J. Am. Chem. Soc.*, 1975, **97**, 1358.
11 (*a*) S. E. Biali and Z. Rappoport, *J. Am. Chem. Soc.*, 1984, **106**, 477; (*b*) D. A. Nugiel, S. E. Biali and Z. Rappoport, *J. Am. Chem. Soc.*, 1989, **111**, 846; (*c*) M. Kaftory, D. A. Nugiel, S. E. Biali and Z.

Rappoport, *J. Am. Chem. Soc.*, 1989, **111**, 8181 and refs. therein; (*d*) G. Klebe, *Struct. Chem.*, 1990, **1**, 597.
12 See, for example, Chatfield and Collins, *Introduction to Multivariate Analysis*, Chapman and Hall, London, 1980.
13 D. A. V. Morton and A. G. Orpen, XIIth European Crystallography Meeting, Moscow, 1989.
14 F. H. Allen, O. Kennard and R. Taylor, *Acc. Chem. Res.*, 1983, **16**, 146; Programs from the Cambridge Crystallographic Data Centre, University Chemical Laboratory, Cambridge; see F. H. Allen and J. E. Davies, in *Crystallographic Computing 4*, eds. N. W. Isaacs and M. R. Taylor, Oxford University Press, Oxford, 1988.
15 P. Murray-Rust and J. Raftery, *J. Mol. Graphics*, 1985, **3**, 50, 60.
16 J. D. Dunitz, *X-Ray Analysis and the Structure of Organic Molecules*, Cornell University Press, Ithaca, NY, 1979.
17 H. C. Longuet-Higgins, *Mol. Phys.*, 1963, **6**, 445.
18 P. Murray-Rust and S. Motherwell, *Acta Crystallogr., Sect. B*, 1978, **34**, 2534.
19 R. Taylor, *J. Mol. Graphics*, 1986, **4**, 123.
20 H.-B. Bürgi and K. C. Dubler-Steudle, *J. Am. Chem. Soc.*, 1988, **110**, 4953, 7291.
21 (*a*) F. H. Allen, M. Doyle and R. Taylor, *Acta Crystallogr., Sect. B*, 1991, **47**, 29, 41, 50; (*b*) F. H. Allen, M. Doyle and T. P. E. Auf der Heyde, *Acta Crystallogr., Sect. B*, 1991, 412.
22 C. Altona, H. J. Geise and C. Romers, *Tetrahedron*, 1968, **24**, 13; C. Altona and M. Sundaralingam, *J. Am. Chem. Soc.*, 1972, **94**, 8205.
23 D. Cremer and J. A. Pople, *J. Am. Chem. Soc.*, 1975, **97**, 1354.
24 S. E. Garner and A. G. Orpen, unpublished work.
25 J. D. Dunitz and H.-B. Bürgi, *Acc. Chem. Res.*, 1983, **16**, 153.
26 J. D. Dunitz and H.-B. Bürgi, *Acta Crystallogr., Sect. B*, 1988, **44**, 445.
27 J. D. Oliver and D. P. Riley, *Organometallics*, 1983, **2**, 1032.
28 K. E. Koenig, in *Asymmetric Synthesis*, ed. J. D. Morrison, Academic Press, Orlando, 1985, vol. 5, ch. 3, p. 71.
29 See J. Halpern, in *Asymmetric Synthesis*, ed. J. D. Morrison, Academic Press, Orlando, 1985, vol. 5, ch. 2, p. 41 and refs. therein.

Received 4*th June* 1991; *Paper* 1/02658E